

Article

High-Density Communities and Infectious Disease Vulnerability: A Built Environment Perspective for Sustainable Health Development

Yue Hu ¹, Ziyi Lin ¹, Sheng Jiao ^{1,2,*} and Rongpeng Zhang ^{1,2,3,*} 

¹ School of Architecture and Planning, Hunan University, Changsha 410082, China; huyue66@hnu.edu.cn (Y.H.); linziyi@hnu.edu.cn (Z.L.)

² Hunan Key Laboratory of Sciences of Urban and Rural Human Settlements in Hilly Areas, Hunan University, Changsha 410082, China

³ Hunan International Innovation Cooperation Base on Science and Technology of Local Architecture, Changsha 410082, China

* Correspondence: jiaosheng2008@163.com (S.J.); zhangrongpeng@hnu.edu.cn (R.Z.)

Abstract: High-density communities have proliferated globally during rapid urbanization. They are characterized by a high population density and limited per capita public spaces, making them susceptible to infectious disease risks. The impact of infectious diseases in these communities, as evident during the COVID-19 pandemic, underscores their vulnerabilities. Yet, research on disease prevention in high-density areas remains limited. This study aims to investigate the relationship between the built environment and the transmission of infectious diseases in high-density urban communities, with a particular focus on the lessons learned during the COVID-19 pandemic. Utilizing Shenzhen city as a case study, this study collected data on the built environment and epidemic trends and involved a generalized linear regression analysis, aiming to understand the key built environment factors that affect epidemic spread in high-density areas. The results from the study revealed that high-density communities experience higher rates of infectious disease transmission compared to their medium- to low-density counterparts. The significant factors identified include land use mixture and walkability, with land use mixture showing the most substantial impact on infection rates. Through a combination of qualitative analysis and empirical research, we constructed a conceptual framework linking containment measures, non-pharmaceutical interventions, and the built environment. The findings emphasize the significance to focus on the health development of high-density communities and offer valuable insights for tailored urban planning and built environment design. These insights are crucial for promoting the healthy and sustainable transformation of existing high-density communities.

Keywords: built environment; high-density community; epidemic infection; healthy; sustainable



Citation: Hu, Y.; Lin, Z.; Jiao, S.; Zhang, R. High-Density Communities and Infectious Disease Vulnerability: A Built Environment Perspective for Sustainable Health Development. *Buildings* **2024**, *14*, 103. <https://doi.org/10.3390/buildings14010103>

Academic Editor: Pablo Pujadas Álvarez

Received: 8 December 2023

Revised: 26 December 2023

Accepted: 28 December 2023

Published: 30 December 2023



Copyright: © 2023 by the authors. Licensee MDPI, Basel, Switzerland. This article is an open access article distributed under the terms and conditions of the Creative Commons Attribution (CC BY) license (<https://creativecommons.org/licenses/by/4.0/>).

1. Introduction

Since the 20th century, cities have been significantly impacted by recurrent outbreaks of infectious diseases [1]. These recurring global outbreaks underscore the fact that cities have become epicenters for disease transmission [2]. Infectious diseases such as AIDS, SARS, HPAI H5N1, and COVID-19 have wrought unprecedented consequences on human health, social stability, and economic progress [3]. The confluence of urbanization and globalization has amplified population mobility and substantial migration to urban centers, creating favorable conditions for the spread of infectious diseases [4,5]. In this context, the community, as a fundamental unit within cities, plays a pivotal role in pandemic preparedness and response. In the post-pandemic era, urban planning aimed at curbing community transmission and fostering the development of resilient and healthy communities has become paramount.

between the floor area ratio (FAR), building density (BD), and COVID-19 transmission remains contentious. Some researchers assert that high FAR and BD values contribute to higher population densities [17,18] and poor ventilation [13], consequently heightening the virus exposure risk. Conversely, others posit that stringent Non-Pharmaceutical Interventions (NPIs) can curtail COVID-19 transmission within high-density communities [19,20]. For instance, during the COVID-19 pandemic, businesses have adjusted their recruitment strategies and the nature of new positions in response to the challenges posed by remote work and the pandemic [21]. Likewise, the correlation between walkability (WB) and COVID-19 transmission has sparked debate. While certain studies suggest that high community WB promotes physical activity, thereby reducing infection risk [22,23], other research underscores the challenge of maintaining social distancing within highly developed urban areas [24,25]. Various community facilities are closely correlated with resident behavior and influence epidemic spread. Elevated-density commercial facilities may lead to overcrowding [19,26], whereas high-density healthcare establishments may heighten the risk of case clustering during consultations [27–29]. Furthermore, convenient public transportation can enhance community mobility and consequently elevate exposure risk [30–32].

Although the specific directional significance of different BE attributes in COVID-19 infection remains unresolved, the significant role of community BEs in COVID-19 prevention and control is well recognized. Yet, most studies have focused predominantly on general communities, with limited attention paid to an in-depth analysis of high-density communities. In such communities, the high population density poses additional challenges for effective residential management, potentially exacerbated by an excessive FAR, which can compromise living conditions, reduce the per capita green space, and diminish natural lighting [33]. Such unique challenges may impact COVID-19 control strategies within high-density communities.

To realize post-pandemic health-oriented community development, a focused analysis of high-density communities is imperative. Our primary goal is to comprehend the impact of the BE within high-density communities on infectious disease transmission, especially in comparison to low-density communities. Our secondary aim involves exploring the correlation between BE factors, such as land use and BD, and the spread of epidemics, while evaluating their potential implications for public health.

This study, based on a review of the literature on epidemics and BEs, presents a framework for BE elements that are integral to community epidemic prevention. Using Shenzhen city as a study case, we utilize a combination of spatial analysis in various dimensions and quantitative calculations to compare high-density communities with regular communities. Through the application of Generalized Linear Models (GLMs), we quantitatively assess the differences in the BE factors that may affect epidemic transmission between high-density and general communities.

We hypothesize that specific BE factors within high-density communities exhibit a significant correlation with the transmission of infectious diseases, potentially resulting in higher infection rates. In conclusion, this research integrates its findings into an analytical framework that encompasses containment measures, NPI, and various pathways involving the BE. The results of this study offer valuable guidance and technical support for the development of new high-density communities and the improvement of existing ones. This research contributes to enhancing the preparedness and control measures against unforeseen public health events.

2. Methods

In the analysis of COVID-19 infection within communities, it is crucial to recognize the multifaceted nature of the BE and its potential impact. Focusing solely on a single level of BE analysis when assessing its influence on COVID-19 infection in communities may lead to biased and incomplete findings, overlooking localized and specific factors. To address this issue, our study initially conducted a statistical analysis of existing empirical

research to identify key indicators of the BE that may influence the transmission of the virus within communities. To further investigate the relationship between these indicators and community infection rates, we conducted a preliminary correlation analysis in the typical high-density city of Shenzhen. However, it is essential to note that this pairwise correlation analysis does not account for potential interactions between variables. To address this limitation, all relevant variables will be further incorporated into a GLM. This will allow us to separately examine the effects of multiple independent variables on the dependent variable, both at the scales of ordinary communities and high-density communities. Furthermore, we will utilize the significance test results (p -values) and standardization coefficients (β) of independent variables to assess the importance of each indicator in influencing the community's epidemic spread.

2.1. Index Selection

Table 1 presents the results of 21 empirical studies examining the relationship between the BE and epidemics in general communities, with investigated indicators classified according to the five “5D” elements of the BE [34].

Table 1. Built environment factors influencing the prevention and control of new crown pneumonia outbreaks in the community.

Authors	Density		Diversity		Design		Destination Accessibility			Distance to Transit
	BD	FAR	LUM	RD	WB	OD	D_cf	D_h	D_gs	D_pt
Behram Wali [35]			-		-	+				
Shakil Bin Kashem et al. [36]			+		-	-			0	
Quynh C. Nguyen [25]					+					
Tianming Zheng [20]	-	-					+	+	+	
Wu Li et al. [32]	+		-	+					-	+
Xin Huang [37]	+						+	+	-	
Tribby and Hartmann [22]					-				0	
Niu et al. [38]	+	+					+		-	+
Credit [28]					-			+		
Guo, Yu and Zhang [23]					-				-	
Asfour [39]						+				
DiMaggio [40]	+									
Rahman [27]				0				+		+
Yong Xu et al. [41]	+			+			+	+		
Bo Li et al. [31]							+	+		+
Emre Tepe [42]							+			
Zerun Liu et al. [43]		-	-				+	-		
Jingwei Wang [19]		-					+	-		-
Eric Gaisie [44]							+			+
Kate H. Choi [45]					-		+			
Dennis Schmiede [46]							-		-	

The direction of association was coded as '+', '-', or '0'; '+' indicates a statistically significant positive association, while '-' represents a statistically significant negative association, and '0' indicates no significant association.

Based on previous reviews, a characteristic of the BE is considered to have strong evidence if the number of positive/negative associations is greater than or equal to the sum of its negative/positive or inconclusive associations [47]. The table shows that there is strong evidence of a positive association between virus infection risk and BD, open design (OD), densities of commercial facilities (D_cf), densities of hospitals (D_h), and densities of public transportation (D_pt). Negative associations with infection risk were found for FAR, land use mixture (LUM), and WB. The evidence for associations of infection risk with other BE factors (e.g., road density and densities of green space) was weak. Notably, scholars have identified that BD, LUM, WB, D_cf, D_h, and D_pt are significantly associated with

COVID-19 infection, and thus, they were selected as the six major BE factors to be further investigated regarding their impacts on COVID-19 infections in high-density communities.

To accurately model and interpret the data, the COVID-19 incidence rate defined as the ratio of COVID-19 cases to the total population of the community was chosen as the dependent variable in this study. This variable was selected due to its ability to consider the population base of each community, and thus, it provides a more precise measure of the probability of infection occurring within a specific population. In terms of independent variables, the study considers various BE indicators, including BD, LUM, WB, D_cf, D_h, and D_pt.

2.2. Theoretical Overview

Within communities, the transmission dynamics of many infectious diseases are intricately linked to human mobility patterns and social interactions, which are factors that are intimately tied to the characteristics of the BE [11]. The BE elements are associated with the features of epidemic transmission, affecting transmission rates through ventilation and congregation dynamics [48,49]. Concurrently, community BE plays a role in controlling infection sources (like home isolation), cutting transmission routes (such as community closures), and offering relief and treatment options [50].

Notably, indoor airborne transmission significantly contributes to COVID-19 infections, especially in congested and poorly ventilated environments [51]. Key elements within the built environment—such as healthcare facilities, retail spaces, cultural hubs, green areas, and transportation networks—serve as pivotal areas for intervening in public spaces, impacting congregation and necessitating focus when devising epidemic prevention strategies [52]. The quantity and scale of these elements can shape congregation dynamics, warranting specific attention to be paid to prevention strategies. Vital preventive measures like physical distancing and population lockdowns remain pivotal [53].

COVID-19 transmission can occur via airborne means or direct/indirect contact within built environments, intricately entangled with human behavior, thus influencing epidemic prevention and control strategies [54]. Our research focuses on analyzing the BE factors influencing epidemic transmission within high-density communities and combining spatial intervention measures to chart the trajectory of health-oriented development in such areas.

2.3. Research Region and Data Sources

Large cities typically pose a higher risk for the transmission of infectious diseases due to the following characteristics: high population density, diversity in residents' health statuses, frequent interpersonal interactions, and a high level of population mobility [55]. Therefore, this study focused on Shenzhen, which was chosen as a representative case due to its high population density and rapid urbanization. Shenzhen is situated in the south-eastern coastal region of Guangdong Province, China and is adjacent to Hong Kong. This vibrant city is divided into 9 districts, encompassing 74 sub-district offices and 677 communities (Figure 2), covering a total area of 1997.47 km² with a resident population of 17,681,600 [56]. The city's extensive urbanization has led to the creation of numerous high-density community units, as evidenced by a growing trend in this direction [57]. Notably, Shenzhen's communities exhibit a distinct dual status characterized by a juxtaposition of urban villages and modern residential buildings, exemplifying typical traits of high population density, a substantial influx of migrants, and a youthful demographic profile.

From 26 February to 16 September 2022, data collected from the Shenzhen Government Data Open Platform revealed 2128 confirmed indigenous COVID-19 cases [58]. Demographic information on local communities was retrieved from official sub-district office websites [59], facilitating the computation of the incidence of COVID-19 per community. The BE data used were gathered from the collection and processing of multivariate big data and vectorized grid maps. Our data extraction strategy included obtaining various Points of Interest (POIs) and Areas of Interest (AOIs) data from Baidu Maps, building outline and height data from Gaud map data, road data from the OpenStreetMap database, and

community boundary data from the Shenzhen Municipal Planning and Natural Resources Bureau's Shenzhen City Map (Outline Version III).

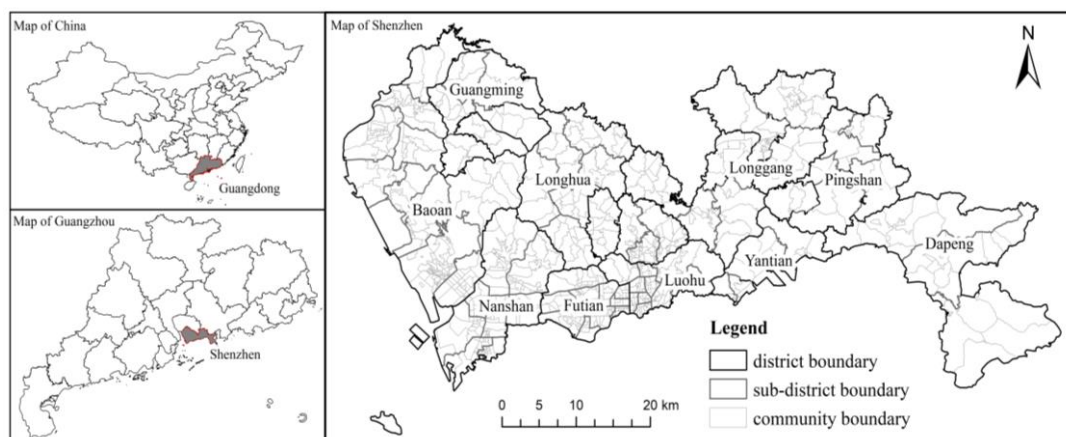


Figure 2. Context map of Shenzhen.

2.4. Statistical Analyzing

To investigate the impacts of these BE factors on COVID-19 infection rates, we employed a three-step statistical analysis (Figure 3). First, we cleaned the case data and obtained data for 311 infected communities in Shenzhen, including the incidence rates, through spatial processing using ArcGIS. Next, we processed the collected BE data, resulting in 6 BE indicators. In the third step, we used the `qcc.overdispersion.test` function in R language to perform an Equi dispersion test on the dependent variable [60], and the results indicate that the distribution of COVID-19 infections within the community is excessively dispersed, and multiple factors within the BE can potentially influence their spread. For our initial analysis, we performed Pearson and Spearman correlation analyses to identify the built environmental influences on epidemic spread in communities. Subsequently, we assessed multicollinearity using variance inflation factors (VIFs). Finally, we utilized Generalized Linear Models (GLMs), including the Poisson model (PM), negative binomial model (NBM), and zero-truncated models (ZTM), as they are better suited for modeling discrete data.

2.4.1. Calculation of Indicators

Six indicators were selected as independent variables in the present study: BD, LUM, WB, D_cf, D_h, and D_pt. The measurement methods for these BE indicators are outlined in Table 2.

In terms of BD, we obtained Shenzhen's building outline data from Baidu Maps and calculated the BD for each community by dividing the base area of community buildings by the community's land area.

In terms of LUM, it can be measured using the entropy index, with values ranging from 0 to 1. When the proportions of different land uses within the study unit are equal, the index is 1 [61]. We obtained AOI (Area of Interest) data for Shenzhen from Baidu Maps to examine the degree of mixture of eight land uses within each community's boundaries: residential; commercial and office; commercial shopping; scientific, educational, cultural and health; public green space; industrial; transportation; and other land uses.

In terms of WB, we obtained data from OpenStreetMap, including 1024 pedestrian and bicycle lanes within the confirmed communities. These data provided information on road categories, road lengths, and geographic locations. WB was calculated as the length of pedestrian and bicycle lanes within the community divided by the community's area.

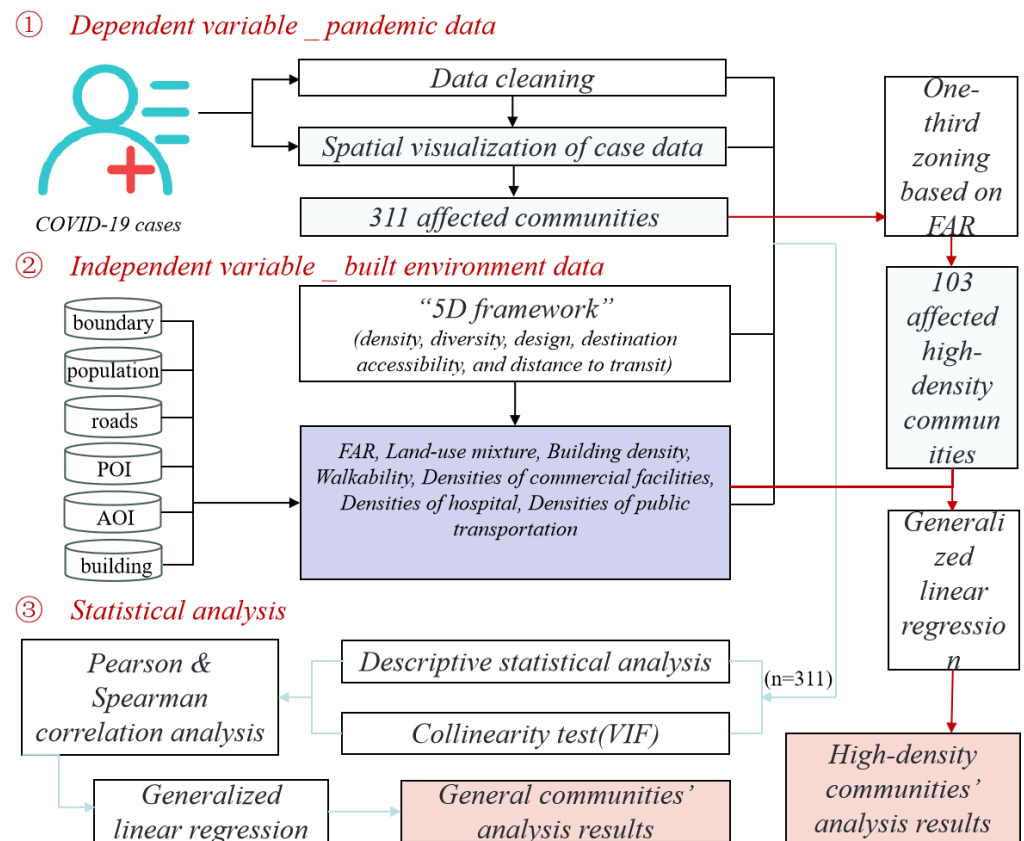


Figure 3. Data analysis workflow diagram.

In terms of facility accessibility, research has shown that the more public service facilities per unit area, the closer the facilities, indicating higher accessibility [17,36]. In this study, we obtained POI data for confirmed communities in Shenzhen from Baidu Maps, including 150,514 commercial facilities, 3773 medical facilities, and 3529 public transportation stops. Accessibility was measured as the number of facilities per square kilometer within each community's boundaries.

Table 2. Built environment metrics used in this study.

Indicator Name	Formula	Description	Data Source
BD	$BD = \frac{BA}{CA}$	BD represents the building density, BA represents the base area of the community building, and CA represents the footprint of the community.	BA: Shenzhen's building outline data from Baidu Maps; CA: Shenzhen Municipal Planning and Natural Resources Bureau's Shenzhen City Map (Out-line Version III)
LUM	$LUM = -\sum pk \ln(pk) \ln(N)$	pk represents the percentage of sites within K in each community, and N is the number of site types in the community.	AOI: Area of Interest data for Shenzhen from Baidu Maps; N: the number of AOI types
WB	$WB = \frac{Lfw + Lcw}{CA}$	The width of sidewalk/bicycle lane is assumed to be normal. Lfw represents the length of the sidewalk in the community, Lcw represents the length of the bike lane in the community, and CA represents the footprint of the community.	The width of sidewalk/bicycle lane: obtained data from OpenStreetMap

Table 2. Cont.

Indicator Name	Formula	Description	Data Source
D_cf	$D_{cf} = \frac{N_{cf}}{CA}$	Ncf represents the number of commercial facilities in the community, and CA represents the footprint of the community.	POI data obtained from Baidu Maps, including 150,514 commercial facilities, 3773 medical facilities, and 3529 public transportation stops
D_h	$D_h = \frac{N_s}{CA}$	Nh represents the number of medical facilities in the community, and CA represents the footprint of the community.	
D_pt	$D_{pt} = \frac{N_{ps}}{CA}$	Nps represents the number of public transportation stops in the community, and CA represents the footprint of the community.	

2.4.2. Correlation Analysis

The Pearson correlation coefficient, also known as the Pearson product moment correlation coefficient, is the most widely used measure of correlation in statistical analysis. It assesses the degree of linear association between two variables, X and Y , assuming that both variables are normally distributed. For binary or other non-normally distributed data, Spearman's correlation analysis is a preferred method, as it employs monotonic functions to evaluate the correlation without relying on the overall distribution or sample size of the data and is less sensitive to outliers. However, the disadvantage of Spearman's method is its lower efficiency compared to Pearson's method. Therefore, it is recommended to consider both Pearson's and Spearman's coefficients, considering the nature and distribution of the data.

The formula for the Spearman correlation coefficient is as follows (1):

$$r = \frac{\sum(X - \bar{X})(Y - \bar{Y})}{\sqrt{\sum(X - \bar{X})^2 \sum(Y - \bar{Y})^2}} \quad (1)$$

Here, X and Y are the values of the two variables, and \bar{X} and \bar{Y} represent their respective means.

The formula for the Spearman correlation coefficient is as follows (2):

$$\rho = 1 - \frac{6\sum d^2}{n(n^2 - 1)} \quad (2)$$

where d represents the differences between ranks, and n is the number of data points.

2.4.3. Regression Analysis

The GLM is an extension of the general linear model that allows us to create regression models for various types of response variables, including count, binary, proportions, and positive-valued continuous distributions. The GLM equation encompasses this flexibility and can be expressed as follows (3):

$$g\{E(y)\} = LP = a + b_1x_1 + b_2x_2 + \dots + b_px_p \quad (3)$$

where $g\{\}$ represents a linear function of the regressors, $E(Y)$ represents the expected value, LP indicates the linear predictive value, a is the constant of the regression equation, x_1, \dots, x_p represent the p environmental variables, and b_1, \dots, b_p are the p regression coefficients.

The Poisson distribution is the most commonly used approach for modeling count data, and it represents a special case of the GLM framework that requires the mean and

variance to be equal [23]. However, in real-world scenarios, data can be overly discrete. For this reason, NBM is better suited for such cases and can result in improved fitting [62]. In the NBM, the variance is assumed to be a quadratic function of the mean [63]. Since we collected communities with COVID-19 infections, where the IR is not zero, the ZTM was used to model count data where the value of zero cannot be observed and if there is evidence of overdispersion [64]. The effectiveness of our model was assessed using four indicators: deviance, AIC value, AICc value, and BIC. A model with lower AIC and AICc values is considered to be better fitted when the difference between the AIC and AICc values of two models is more than or equal to 3 [65]. The statistical analyses were performed using R software (V.4.0.4), with the MASS and pscl packages employed.

3. Results

3.1. Spatial Patterns of COVID-19 Infections and BEs in Shenzhen Communities

We performed a spatial analysis of the 2128 COVID-19 cases, using ArcGIS software to visualize their distribution across 341 communities in Shenzhen (Figure 4). Among these, the Futian District recorded the highest cumulative number of cases, with 1091 cases, representing 51.2% of the total. Following closely were the Luohu District and Nanshan District, with 241 (11.3%) and 292 cases (13.7%), respectively, primarily concentrated in the southwestern region of Shenzhen. On the other hand, the Dapeng New District and Guangming District each reported only three cumulative cases, while Pingshan District had just two cases, ranking them as the top three districts with the most effective epidemic control. These districts are situated in the eastern and northwestern areas of Shenzhen. To gain a more comprehensive insight into the distribution of infection cases, we conducted COVID-19 kernel density analyses based on both population and area in the ArcGIS software (refer to Figure 4b,c). The distribution patterns revealed overall consistency with the spatial distribution of case numbers. Hotspots remained concentrated in the Futian District, Luohu District, and Nanshan District. However, when considering the population density, the Nanshan District exhibited a notably higher infection rate. Conversely, coldspots were identified in the western areas, particularly in the Dapeng New District and Pingshan District.

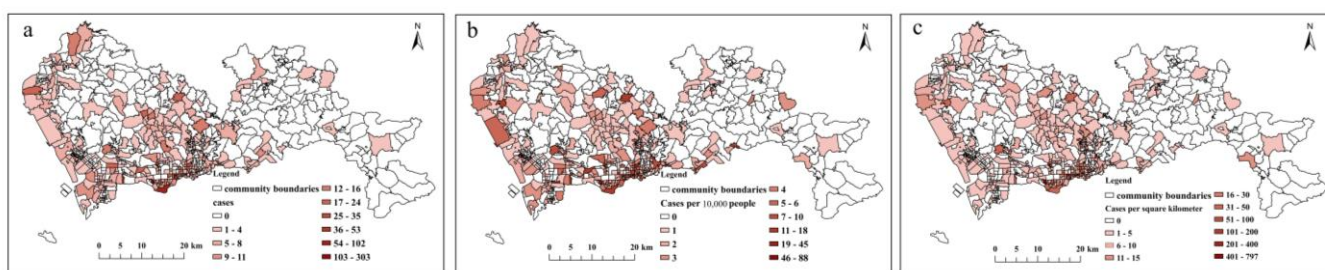


Figure 4. Distribution of locally confirmed cases in Shenzhen communities. (a) COVID-19 cases in communities; (b) COVID-19 cases per 10,000 people in communities; (c) COVID-19 cases per square kilometer in communities.

Furthermore, we conducted an in-depth exploration of the spatial distribution of BEs in the infected communities of Shenzhen, encompassing parameters such as population density, FAR, BD, LUM, WB, D_h, D_{cf}, and D_{pt} (Figure 5). The spatial distribution analysis of the BE factors yielded several significant findings. Firstly, all hotspots for the distribution of BEs were concentrated in the Futian District, Luohu District, and Nanshan District, whereas coldspots were evident in the Dapeng New District and Pingshan District. Secondly, we observed significant variations in the kernel density distribution of medical facilities, commercial facilities, and transportation hubs. These factors exhibited distinct spatial patterns, reflecting their varied concentrations and accessibility across the city. Thirdly, when considering LUM and WB, we found them to exhibit intermediate patterns in their spatial distributions. These factors were less concentrated in the central districts

(Futian, Luohu, and Nanshan) compared to medical facilities, commercial establishments, and transportation hubs. Lastly, the population density, FAR, and BD demonstrated a relatively smaller presence and a more uniform distribution across the city.

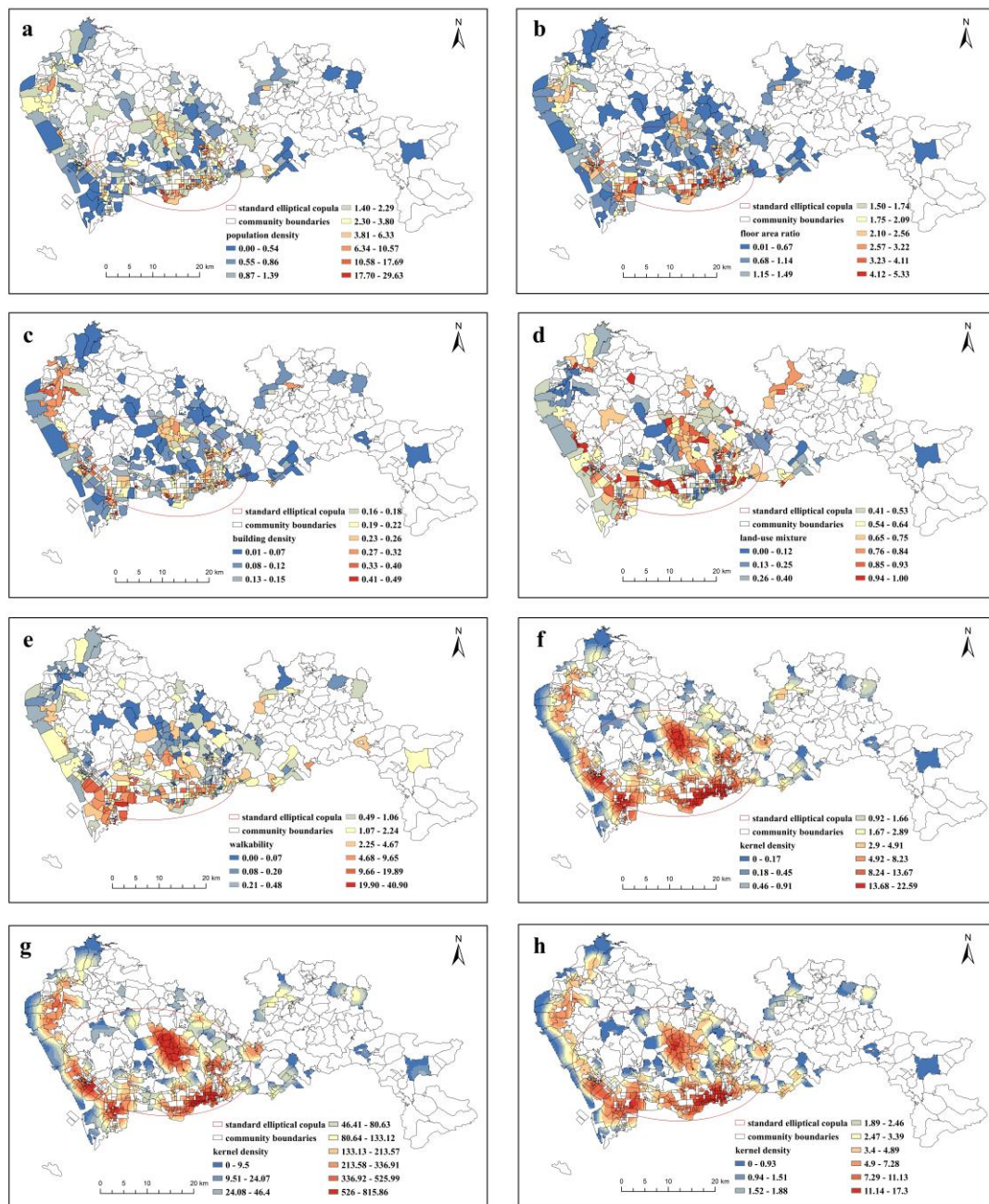


Figure 5. Spatial distribution of BEs in eight types of communities ((a) population density; (b) floor area ratio; (c) building density; (d) land use mixture; (e) walkability; (f) medical facilities; (g) commercial facilities; (h) public transportation).

It is imperative to acknowledge that while our spatial analysis has unveiled these distinctive patterns, there remains a critical need for additional quantitative investigations to elucidate the intricate relationships between infection rates and these specific BEs. This essential next step will yield a more refined comprehension of how the community BEs may influence the transmission of infectious diseases, including COVID-19. Subsequently, the insights gained from such analyses can serve as valuable guidance for the formulation of precise urban planning strategies and informed public health interventions.

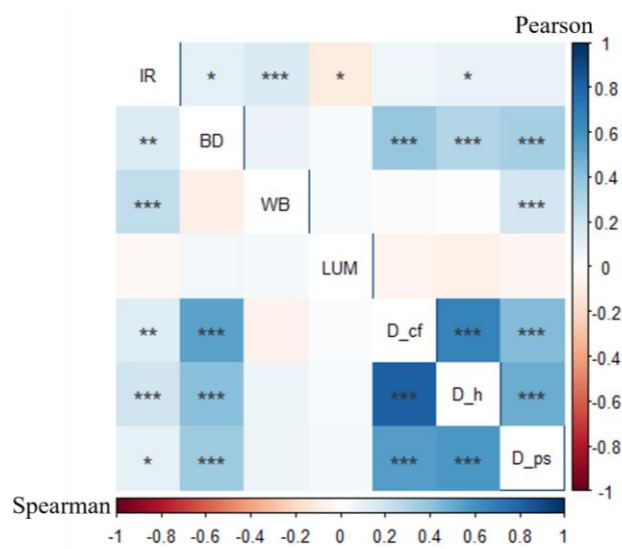
3.2. Relationship between the Community Epidemic Incidence and Built Environment

Following the exclusion of communities with incomplete data, our analysis focused on 311 case communities. This paper used a correlation analysis to determine the BEs that influence community COVID-19 infection. Table 3 shows the descriptive statistical results of the indicators of the community's BEs. The correlations between community COVID-19 incidence and six explanatory variables were determined using Pearson and Spearman correlation coefficients before conducting specific regression modeling. In general, we found large differences in the associations between the variables and COVID-19 in the community, with a range of 0.03–0.26, indicating that different BEs differed significantly in the importance of the impact of the epidemic (Figure 6).

Table 3. Descriptive statistical analysis of built environment factors and correlation coefficient statistics.

Variable	Descriptive Statistics		Pearson		Spearman		Collinearity	
	Mean	Std. Dev.	Coef.	<i>p</i> -Value	Coef.	<i>p</i> -Value	VIF	1/VIF
BD	0.199	0.097	0.1048 *	0.0650	0.1412 **	0.0127	1.24	0.807
LUM	0.570	0.293	−0.1033 *	0.0689	−0.0318	0.5758	1.01	0.989
WB	2.860	4.594	0.1512 ***	0.0076	0.2430 ***	<0.001	1.05	0.948
D_cf	529.794	641.605	0.0658	0.2476	0.1375 **	0.0152	1.95	0.513
D_h	14.350	16.053	0.0968 *	0.0885	0.1934 ***	<0.001	1.99	0.503
D_pt	10.607	9.940	0.0916	0.1067	0.1009 *	0.0755	1.48	0.675

* $p < 0.1$; ** $p < 0.05$; *** $p < 0.01$.



* $p < 0.1$; ** $p < 0.05$; *** $p < 0.01$.

Figure 6. Pearson and Spearman correlation matrix plot.

The selection of the α critical value in hypothesis testing should be based on the specific context. Normally, values such as $\alpha = 0.01$, 0.05 , or 0.1 are used, corresponding to probabilities of correctly accepting the null hypothesis at 99%, 95%, or 90%, respectively [66]. Our Pearson and Spearman correlation analyses identified three environmental factors that were significantly associated with community morbidity: WB ($p < 0.01$), D_h ($p < 0.1$), and BD ($p < 0.1$). However, three other factors, specifically LUM (Ppearson = 0.5758, Pspearman = 0.5758), D_cf (Ppearson = 0.2476, Pspearman < 0.05), and D_pt (Ppearson = 0.1067, Pspearman < 0.1), displayed different levels of association with community morbidity between the two correlation analyses. To avoid any issues of excessive multicollinearity among the six selected explanatory variables, we employed the variance inflation factor (VIF) test, which did not reveal concerns of collinearity (VIF < 10) [67].

The results of our correlation analysis indicated that the significance of the BEs we examined with regard to COVID-19 infection varied, which may be attributed to the distribution characteristics of the data. To enhance the accuracy of our analysis, we employed various methods and compared the fitting effects of different models.

3.3. GLM Regression Results for General Communities

In this study, we conducted PM, NBM, and ZTNBM regression analyses on a sample of 311 communities. Table 4 presents the results of our regression analyses regarding BEs that influence community epidemic transmission. The Negative Binomial_F model demonstrated a higher level of explanation, as evidenced by the lower values of the Deviance, AIC, AICc, and BIC, respectively. Our findings suggest that three indicators were significantly and positively associated with community epidemic transmission, which were BD, WB, and D_h, while LUM was negatively associated. The regression coefficients revealed that the impact of BD (1.685) on community epidemic transmission was the most significant, while the impact of D_h (0.012) was found to be the least significant. WB (0.055) and LUM (−0.738) instead exhibited moderate impacts.

Table 4. GLM regression results for general communities.

Variable	Poisson_F			Negative Binomial_F			Zero Truncated nb_F		
	Estimate	S.E.	<i>p</i>	Estimate	S.E.	<i>p</i>	Estimate	S.E.	<i>p</i>
Intercept	3.100 ***	0.033	<0.001	0.701 ***	0.204	<0.001	2.781 ***	0.252	<0.001
BD	1.671 ***	0.122	<0.001	1.685 **	0.766	0.027	1.846 **	0.916	0.044
WB	0.044 ***	0.002	<0.001	0.055 ***	0.014	<0.001	0.064 ***	0.021	0.002
LUM	−0.739 ***	0.036	<0.001	−0.738 ***	0.229	0.001	−0.767 ***	0.264	0.004
D_h	0.012 ***	0.001	<0.001	0.012 **	0.006	0.029	0.013 *	0.007	0.052
D_cf	−0.000 **	0.000	0.032	−0.000	0.000	0.664	−0.000	0.000	0.533
D_pt	−0.005 ***	0.001	<0.001	0.000	0.008	0.970	0.002	0.009	0.817
Deviance		13,972.62			370.603			2573.4	
AIC		15,343.665			1323.309			2589.388	
AICc		15,344.035			1323.786			2589.865	
BIC		15,369.844			1353.227			2619.306	

* $p < 0.1$; ** $p < 0.05$; *** $p < 0.01$.

3.4. GLM Regression Results for High-Density Communities

We initiated a group analysis on the processed data, dividing communities with COVID-19 cases into three categories based on the FAR (Figure 7): high-density, medium-density, and low-density communities. The results indicate that high-density communities exhibit significantly higher values for average case numbers, average incidence rates, and cumulative diagnosis densities compared to medium- and low-density communities, with the disparities being twice as large. These findings strongly emphasize the substantially elevated risk of epidemic infection in high-density communities, highlighting the critical need for focused attention in this regard.

We conducted a regression analysis on the group of 103 high-density communities obtained after grouping, and the results of this analysis are presented in Table 5. Among the three models, PM_H has the highest deviance, AIC, AICc, and BIC values. Therefore, PM_H is initially excluded. The AIC, AICc, and BIC are designed to balance the goodness of fit and complexity of the models, penalizing model complexity to prevent overfitting. In the comparison between NBM_H and ZTNBM_H, NBM_H exhibits significantly lower deviance than ZTNBM_H, indicating its superiority in fitting the data. AIC, AICc, and BIC are slightly higher for NBM_H compared to ZTNBM_H, suggesting that NBM_H may be more complex; hence, NBM_H is selected. This led us to conclude that LUM ($p = 0.009$) and WB ($p = 0.047$) displayed high levels of significance. Specifically, LUM demonstrates a significant negative correlation, while WB shows a positive correlation with the absolute value of the correlation coefficient, as the LUM value is greater than that for WB.

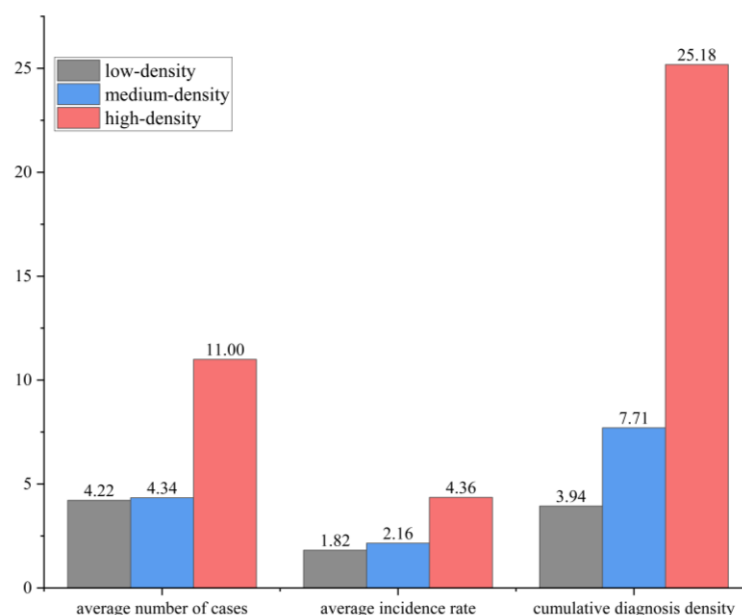


Figure 7. Epidemic situation in low-, medium-, and high-density communities in Shenzhen.

Table 5. GLM regression results for high-density communities.

Variable	Poisson_H			Negative Binomial_H			Zero Truncated nb_H		
	Estimate	S.E.	<i>p</i>	Estimate	S.E.	<i>p</i>	Estimate	S.E.	<i>p</i>
Intercept	4.250 ***	0.069	<0.001	3.873 ***	0.506	<0.001	3.797 ***	0.492	<0.001
BD	0.530 **	0.225	0.018	1.072	1.511	0.489	1.123	1.784	0.529
WB	0.039 ***	0.002	<0.001	0.039 **	0.020	0.047	0.041	0.025	0.105
LUM	−1.140 ***	0.049	<0.001	−1.010 ***	0.347	0.004	−1.066 ***	0.412	0.009
D_h	0.000	0.000	0.904	0.001	0.001	0.466	0.006	0.008	0.478
D_cf	0.000	0.000	0.330	0.000	0.000	0.878	0.000	0.000	0.835
D_pt	−0.016 ***	0.001	<0.001	−0.014	0.010	0.167	−0.014	0.011	0.197
Deviance		7582.157			118.576			950	
AIC		8091.276			977.801			965.963	
AICc		8092.455			979.333			967.495	
BIC		8109.719			998.879			987.041	

* $p < 0.1$; ** $p < 0.05$; *** $p < 0.01$.

4. Discussion

4.1. Analysis of Shenzhen's Epidemic Distribution Patterns and BE Characteristics

By combining the epidemic distribution characteristics in Shenzhen (Figure 4) with the spatial distribution of FAR (Figure 5b), we observed that regions with severe outbreaks often corresponded to areas with a high FAR. Furthermore, by quantifying the infection rates in communities of different densities, we found that high-density communities had infection rates more than twice as high as those in medium- and low-density communities (Figure 7). This underscores the significant risks associated with high-density communities during epidemic outbreaks, highlighting the need for focused attention in epidemic prevention and control management as well as in health planning.

The spatial distribution of BE factors in Shenzhen also reveals the distinctiveness of its high-density areas (Figure 5). Specifically, the analysis reveals that central urban areas, characterized by a high population density and intensified urban development, exhibit a more substantial presence of various BE elements. These encompass critical components such as medical facilities, commercial establishments, and transportation hubs. What is particularly noteworthy is the pronounced disparities observed between hotspots and coldspots across these categories. This disparity underscores a key point: specific elements

of the BE, including healthcare infrastructure, commercial amenities, and transportation networks, tend to be disproportionately concentrated in high-density communities, making high-density communities more conducive to prevention and control efforts to some extent.

4.2. Built Environment Factors Affecting COVID-19 Cases in High-Density Communities

High-density BEs are characterized by several key features, including spatial high-intensity development, three-dimensional transportation organization, high-density multi-functionality, frequent population interactions, interwoven underground spatial networks, and challenging outdoor physical conditions [10]. These attributes have substantially exacerbated the spread and diffusion of diseases due to the highly concentrated population and interconnected urban networks associated with high-density BEs.

Our study identified LUM and WB as the most significant BEs impacting COVID-19 infection rates in high-density communities, which is consistent with the sign of the correlation analysis results. However, several other factors, including BD, D_cf, D_h, and D_pt, which exhibited significant correlations in the correlation analysis, did not demonstrate substantial effects in the regression analysis. This inconsistency can be attributed to the difference between the correlation analysis, which evaluates the relationship between two variables, and the regression model, which considers the interplay among independent variables.

Interestingly, our analysis revealed a positive correlation between WB and COVID-19 infection rates at the high-density community level. This finding is consistent with a study conducted on COVID-19 infection rates in communities across 20 states in the United States [25]. This suggests that enforcing social distancing measures may be more challenging in densely developed urban areas. Conversely, other research has indicated that pedestrian-oriented streets are associated with lower mortality and hospitalization rates [22,68]. This could be because high walkability encourages physical activity, enhances residents' physical fitness, and thereby reduces the likelihood of infection.

In contrast, LUM exhibited a negative correlation with COVID-19 infection rates, aligning with the findings of the majority of the existing research [38,69]. A higher degree of LUM implies a better spatial proximity of urban services and diverse functions that cater to residents' needs. This results in reduced travel distances and less frequent travel, ultimately lowering the risk of infection due to reduced exposure to traffic-related contagion. The LUM may exert a more significant influence than walkability, as it impacts both travel mode and distance [70]. It increases the probability of the origin and the destination of travelers being within the same vicinity, meeting residents' daily needs during the epidemic, and minimizing non-commuting interactions across communities. In comparison to walkability, it may also decrease residents' likelihood of visiting high-risk areas.

4.3. Comparative Analysis between High-Density Communities and General Communities

The emphasis on maintaining social distancing has emerged as a crucial intervention measure in the prevention of infectious diseases. In China, high-density communities characterized by high floor area ratios have gained prominence as land-saving urban layouts. However, they may not always facilitate effective ventilation and can present certain transmission risks, making them susceptible to disease spread [13]. Our analysis revealed that high-density communities exhibited the highest risk of COVID-19 infection when compared to general communities. In general communities, the key BEs influencing COVID-19 cases included BD, WB, LUM, and D_h. Remarkably, the LUM and WB were significantly associated with COVID-19 cases in both high-density and general communities.

Furthermore, our regression analyses, conducted separately for high-density and general communities, highlighted significant disparities in the impact of various indicators. Notably, BD and D_h lost their significance in high-density communities. These indicators exhibited consistent high values in high-density communities, with minimal variations and no discernible impact on epidemic transmission. These findings underscore the necessity for tailored planning and design strategies based on the density level of the

communities in question. To further extend this discussion, it is essential to consider the broader implications of these findings. High-density communities, which are prevalent in rapidly urbanizing regions, present a unique challenge in disease transmission management. While they often offer benefits in terms of efficient land use, reduced commute times, and proximity to urban amenities, they also entail greater population density and complexity. Therefore, mitigating the transmission risks within high-density communities requires multifaceted strategies.

4.4. Guidance on the Built Environment Design of High-Density Communities

In the context of high-density communities, the discussion around the design of the BE takes on critical significance. Spatial interventions have been a cornerstone in achieving effective epidemic containment, encompassing strategies aimed at isolating infection sources, disrupting transmission pathways, and safeguarding vulnerable populations [71,72]. The conceptual framework, as depicted in Figure 8, illustrates the intricate interplay between containment measures, NPIs, and the BEs of communities. An analysis of the epidemic prevention process reveals that infection sources primarily originate from residents with transmission capabilities, who subsequently construct transmission chains within their living areas [52].

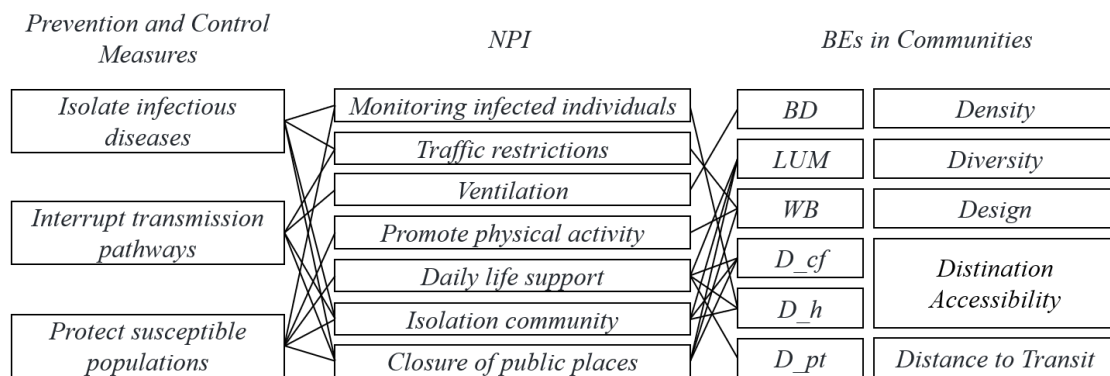


Figure 8. The conceptual framework of various pathways between containment measures, NPIs, and community BEs.

When considering the isolation of infection sources, it becomes evident that grassroots health service institutions within communities play a pivotal role. These institutions are responsible for swift infection testing within the community and the implementation of isolation measures for confirmed cases. The adequacy of medical facility infrastructure, to a certain extent, influences a community's ability to quarantine and isolate individuals affected by novel viruses [73]. Concurrently, NPIs like traffic restrictions, community lockdowns, and the closure of public spaces emerge as indispensable measures. These restrictions limit population movement, both within and beyond the community, effectively reducing the risk of epidemic transmission. In the realm of safeguarding susceptible populations, several measures have proven vital. These include promoting proper ventilation to mitigate aerosol-based infections, encouraging physical activity to enhance overall physical fitness, and providing a diverse array of public facilities within the community to meet residents' daily needs. In high-density communities, optimizing the layout and accessibility of these facilities becomes particularly critical.

Furthermore, the consideration of the LUM and WB takes center stage when designing high-density communities. In essence, communities characterized by a higher degree of LUM are strategically designed to minimize travel distances for their inhabitants. This reduced need for travel results in fewer interactions, ultimately decreasing the risk of infection associated with traffic exposure. Conversely, WB, although generally associated with higher COVID-19 infection rates in high-density communities, requires nuanced consideration. While promoting physical activity through walkability to enhance residents'

physical fitness, planners should consider widening sidewalks or establishing multiple square nodes to increase space and avoid crowding.

Our findings provide new insights and guidance for designing high-density communities and controlling COVID-19 in existing ones. These insights offer valuable guidance for the future development of high-density urban areas, emphasizing the importance of creating resilient, health-conscious environments that are prepared to confront and mitigate the challenges posed by infectious diseases.

5. Conclusions

As urbanization continues to accelerate, with high-density urban areas proliferating rapidly, it becomes increasingly imperative for urban planners and policymakers to acknowledge and address the vulnerabilities that are inherent in the built environment. This study underscores the significant influence of the BE on infectious disease transmission, particularly in high-density communities. Our research, focusing on the emblematic high-density city of Shenzhen, selected six key BE indicators based on the statistical analyses of existing research conclusions. By examining 311 infected communities in Shenzhen and categorizing 103 high-density communities, we combined spatial and quantitative analyses of epidemic infections and BE factors to unravel the extent of the outbreak and the characteristics of the BE elements in high-density communities.

Our findings unequivocally demonstrate a stark contrast between high-density areas and medium- to low-density communities. High-density areas exhibited significantly higher case numbers, incidence rates, and diagnosis density, indicating a heightened risk of epidemic infections. Through a correlation analysis and GLM models, specific BE factors affecting high-density and general communities were identified. In general communities, BD, WB, and D_h were positively correlated, with BD being the most influential. In high-density communities, LUM showed a negative correlation, while WB exhibited a positive correlation, with LUM being the most influential factor. To address the unique challenges of epidemic prevention in high-density areas, our study proposes a comprehensive conceptual framework integrating containment measures, NPIs, and the BE. This framework emphasizes isolating infectious cases, disrupting transmission pathways, and safeguarding vulnerable populations. Our regression analysis emphasizes the critical role of prioritizing land use and walkability in the planning of new or refurbished high-density communities.

This research offers practical implications for enhancing epidemic prevention and control in high-density urban areas, facilitating tailored urban planning and BE design and the healthy and sustainable transformation of existing high-density communities. It is essential to note that the findings and recommendations of this study are specific to the context of the studied region, and their applicability to other geographical locations may vary due to differing socio-economic, cultural, and environmental factors. Future research directions may include delving into the mechanisms of epidemic transmission, considering occupant behavior in diverse climate regions, and examining the resident population composition within communities to achieve a more comprehensive understanding of the factors affecting epidemic transmission.

Author Contributions: Y.H.: Conceptualization, methodology, software, validation, formal analysis, investigation, data curation, writing, and visualization. Z.L.: Validation, formal analysis, resources, data curation, and writing. S.J.: Conceptualization, supervision, project administration, and resources. R.Z.: Conceptualization, methodology, writing, supervision, project administration, and funding. All authors have read and agreed to the published version of the manuscript.

Funding: This research was funded by the Hunan Province Innovation Development Program, grant number 2020TP1009.

Data Availability Statement: Data available in a publicly accessible repository that does not issue DOIs. Publicly available datasets were analyzed in this study. This data can be found via [<https://pan.baidu.com/s/1WJGJt7OVnw644FchmA3rHQ?pwd=9mzq>].

Conflicts of Interest: Author Rongpeng Zhang was employed by the Hunan International Innovation Cooperation Base on Science and Technology of Local Architecture. The remaining authors declare that the research was conducted in the absence of any commercial or financial relationships that could be construed as a potential conflict of interest.

References

1. Pinter-Wollman, N.; Jelić, A.; Wells, N.M. The Impact of the Built Environment on Health Behaviours and Disease Transmission in Social Systems. *Philos. Trans. R. Soc. B Biol. Sci.* **2018**, *373*, 20170245. [CrossRef] [PubMed]
2. Ma, J.; Xu, J.; Zhao, X.; Huo, S.; Duan, X.; Mu, Y.; Wang, Y.; Wei, Y.; Chang, J.; Jin, X.; et al. Several major issues concerning the environmental transmission and risk prevention of SARS-CoV-2. *Sci. China Earth Sci.* **2022**, *65*, 1047–1056. [CrossRef] [PubMed]
3. Wu, X.; Tian, H.; Zhou, S.; Chen, L.; Xu, B. Impact of global change on transmission of human infectious diseases. *Sci. China Earth Sci.* **2014**, *57*, 189–203. [CrossRef] [PubMed]
4. Neiderud, C.-J. How Urbanization Affects the Epidemiology of Emerging Infectious Diseases. *Infect. Ecol. Epidemiol.* **2015**, *5*, 27060. [CrossRef] [PubMed]
5. Woolhouse, M.E.J.; Gowtage-Sequeria, S. Host range and emerging and reemerging pathogens. *Emerg. Infect. Dis.* **2005**, *11*, 1842–1847. [CrossRef]
6. Adams, R.I.; Bhangar, S.; Dannemiller, K.C.; Eisen, J.A.; Fierer, N.; Gilbert, J.A.; Green, J.L.; Marr, L.C.; Miller, S.L.; Siegel, J.A.; et al. Ten Questions Concerning the Microbiomes of Buildings. *Build. Environ.* **2016**, *109*, 224–234. [CrossRef]
7. Glaeser, E. Cities, Productivity, and Quality of Life. *Science* **2011**, *333*, 592–594. [CrossRef]
8. Bodea, C.N.; Purnus, A. Legal implications of adopting Building Information Modeling (BIM). *Jurid. Trib.-Trib. Jurid.* **2018**, *8*, 63–72.
9. Li, H.; Liu, Z. Temporal and Spatial Evolution of Urban Density in China and Analysis of Urban High Density Development: From 1981 to 2014. *Urban Dev. Studies.* **2019**, *26*, 46–54.
10. Shi, B.; Marvin, S.; Yang, J. Study on Quality Improvement of Built Environment in High-density Urban Areas Under the Background of Post Smart City Transformation. *Urban Plan. Int.* **2021**, *36*, 16–21. [CrossRef]
11. Yao, Y.; Pan, H.; Cui, X.; Wang, Z. Do Compact Cities Have Higher Efficiencies of Agglomeration Economies? A Dynamic Panel Model with Compactness Indicators. *Land Use Policy* **2022**, *115*, 106005. [CrossRef]
12. Correia, S.; Luck, S.; Verner, E. Pandemics Depress the Economy, Public Health Interventions Do Not: Evidence from the 1918 Flu. *J. Econ. Hist.* **2022**, *82*, 917–957. [CrossRef]
13. Wang, Z.; Zhang, Y. Review on the Relationship between High-density Built Environment and Public Health. *South Archit.* **2023**, *6*, 21–31. Available online: <https://kns.cnki.net/kcms/detail/44.1263.TU.20230406.1325.008.html> (accessed on 20 April 2022).
14. Duan, J.; Zhang, J.; Chai, Y.; Zhai, G.; Li, Z.; Tan, Z.; Yang, D.; Yang, J.; Yuan, Y.; Liu, W.; et al. “What lesson does COVID-19 teach planning?” Academic writing. *Urban Plan. Forum.* **2022**, *3*, 1–10. [CrossRef]
15. Allam, Z.; Jones, D.S. Pandemic Stricken Cities on Lockdown. Where Are Our Planning and Design Professionals [Now, Then and into the Future]? *Land Use Policy* **2020**, *97*, 104805. [CrossRef] [PubMed]
16. Deng, L.; Wang, L. The Impact of Urban Expansion and High Density on Infectious Diseases and Planning Strategies. *New Archit.* **2021**, *6*, 88–93. [CrossRef]
17. Li, X.; Zhou, L.; Jia, T.; Peng, R.; Fu, X.; Zou, Y. Associating COVID-19 Severity with Urban Factors: A Case Study of Wuhan. *Int. J. Environ. Res. Public Health* **2020**, *17*, 6712. [CrossRef] [PubMed]
18. Kan, Z.; Kwan, M.-P.; Wong, M.S.; Huang, J.; Liu, D. Identifying the Space-Time Patterns of COVID-19 Risk and Their Associations with Different Built Environment Features in Hong Kong. *Sci. Total Environ.* **2021**, *772*, 145379. [CrossRef]
19. Wang, J.; Zeng, F.; Tang, H.; Wang, J.; Xing, L. Correlations between the Urban Built Environmental Factors and the Spatial Distribution at the Community Level in the Reported COVID-19 Samples: A Case Study of Wuhan. *Cities* **2022**, *129*, 103932. [CrossRef]
20. Zheng, T.; Liu, H. Exploration of the Built-Environmental Elements that Influence the Spread of COVID19 Pandemic on Community Scale: A Case Study of Wuhan, China. *Mod. Urban Res.* **2020**, *10*, 20–29. [CrossRef]
21. Campello, M.; Kankanalli, G.; Muthukrishnan, P. Corporate Hiring Under COVID-19: Financial Constraints and the Nature of New Jobs. *J. Financ. Quant. Anal.* **2023**, *Published online*, 1–45. [CrossRef]
22. Tribby, C.P.; Hartmann, C. COVID-19 Cases and the Built Environment: Initial Evidence from New York City. *Prof. Geogr.* **2021**, *73*, 365–376. [CrossRef]
23. Guo, Y.; Yu, H.; Zhang, G.; Ma, D.T. Exploring the Impacts of Travel-Implied Policy Factors on COVID-19 Spread within Communities Based on Multi-Source Data Interpretations. *Health Place* **2021**, *69*, 102538. [CrossRef] [PubMed]
24. Guan, C.; Tan, J.; Li, Y.; Cheng, T.; Yang, J.; Liu, C.; Keith, M. How do density, employment and transit affect the prevalence of COVID-19 pandemic? A study of 3,141 counties across the United States. *Health Place* **2023**, *84*, 103117. [CrossRef] [PubMed]
25. Nguyen, Q.C.; Huang, Y.; Kumar, A.; Duan, H.; Keralis, J.M.; Dwivedi, P.; Meng, H.-W.; Brunisholz, K.D.; Jay, J.; Javanmardi, M.; et al. Using 164 Million Google Street View Images to Derive Built Environment Predictors of COVID-19 Cases. *Int. J. Environ. Res. Public Health* **2020**, *17*, 6359. [CrossRef] [PubMed]
26. Zhou, W. Research on the Correlation between Urban Built Environment and High-risk Communities under Epidemic Situation Based on the Sample of Seven Urban Communities in Hankou. *New Archit.* **2020**, *6*, 52–55. [CrossRef]

27. Rahman, M.H.; Zafri, N.M.; Ashik, F.R.; Waliullah, M.; Khan, A. Identification of Risk Factors Contributing to COVID-19 Incidence Rates in Bangladesh: A GIS-Based Spatial Modeling Approach. *Heliyon* **2021**, *7*, e06260. [[CrossRef](#)]
28. Credit, K. Neighbourhood Inequity: Exploring the Factors Underlying Racial and Ethnic Disparities in COVID-19 Testing and Infection Rates Using ZIP Code Data in Chicago and New York. *Reg. Sci. Policy Pract.* **2020**, *12*, 1249–1271. [[CrossRef](#)]
29. Wang, L.; Hu, Z.; Zhou, K.; Kwan, M.-P. Identifying spatial heterogeneity of COVID-19 transmission clusters and their built-environment features at the neighbourhood scale. *Health Place* **2023**, *84*, 103130. [[CrossRef](#)]
30. Li, B.; Liu, Q.; He, H.; Peng, Y. The Influence of Urban Built Environment on COVID-19 Epidemic and Its Prevention and Control Measures. *Chin. Overseas Archit.* **2021**, *12*, 2–7. [[CrossRef](#)]
31. Li, B.; Peng, Y.; He, H.; Wang, M.; Feng, T. Built Environment and Early Infection of COVID-19 in Urban Districts: A Case Study of Huangzhou. *Sustain. Cities Soc.* **2021**, *66*, 102685. [[CrossRef](#)] [[PubMed](#)]
32. Li, W.; Zhao, S.-C.; Ji, X.-F.; Ma, J.-W. Impact of Traffic Exposure and Land Use Patterns on the Risk of COVID-19 Spread at the Community Level. *China J. Highw. Transp.* **2020**, *33*, 43–54. [[CrossRef](#)]
33. Duan, J.; Yang, B.; Zhou, L.; Zhang, J. Planning Improves City's Immunity: A Written Conversation on COVID-19 Breakout. *City Plan. Rev.* **2020**, *44*, 115–136.
34. Ewing, R.; Cervero, R. Travel and the Built Environment: A Meta-Analysis. *J. Am. Plann. Assoc.* **2010**, *76*, 265–294. [[CrossRef](#)]
35. Wali, B.; Frank, L.D. Neighborhood-Level COVID-19 Hospitalizations and Mortality Relationships with Built Environment, Active and Sedentary Travel. *Health Place* **2021**, *71*, 102659. [[CrossRef](#)] [[PubMed](#)]
36. Bin Kashem, S.; Baker, D.M.; González, S.R.; Lee, C.A. Exploring the Nexus between Social Vulnerability, Built Environment, and the Prevalence of COVID-19: A Case Study of Chicago. *Sustain. Cities Soc.* **2021**, *75*, 103261. [[CrossRef](#)] [[PubMed](#)]
37. Huang, X.; Yang, Q.; Yang, J. Importance of Community Containment Measures in Combating the COVID-19 Epidemic: From the Perspective of Urban Planning. *Geo-Spat. Inf. Sci.* **2021**, *24*, 363–371. [[CrossRef](#)]
38. Niu, Q.; Wu, W.; Shen, J.; Huang, J.; Zhou, Q. Relationship between Built Environment and COVID-19 Dispersal Based on Age Stratification: A Case Study of Wuhan. *Int. J. Environ. Res. Public Health* **2021**, *18*, 7563. [[CrossRef](#)]
39. Asfour, O.S. Housing Experience in Gated Communities in the Time of Pandemics: Lessons Learned from COVID-19. *Int. J. Environ. Res. Public Health* **2022**, *19*, 1925. [[CrossRef](#)]
40. DiMaggio, C.; Klein, M.; Berry, C.; Frangos, S. Black/African American Communities Are at Highest Risk of COVID-19: Spatial Modeling of New York City ZIP Code-Level Testing Results. *Ann. Epidemiol.* **2020**, *51*, 7–13. [[CrossRef](#)]
41. Xu, Y.; Guo, C.; Yang, J.; Yuan, Z.; Ho, H.C. Modelling Impact of High-Rise, High-Density Built Environment on COVID-19 Risks: Empirical Results from a Case Study of Two Chinese Cities. *Int. J. Environ. Res. Public Health* **2023**, *20*, 1422. [[CrossRef](#)] [[PubMed](#)]
42. Tepe, E. The Impact of Built and Socio-Economic Environment Factors on Covid-19 Transmission at the ZIP-Code Level in Florida. *J. Environ. Manag.* **2023**, *326*, 116806. [[CrossRef](#)] [[PubMed](#)]
43. Liu, C.; Liu, Z.; Guan, C. The Impacts of the Built Environment on the Incidence Rate of COVID-19: A Case Study of King County, Washington. *Sustain. Cities Soc.* **2021**, *74*, 103144. [[CrossRef](#)] [[PubMed](#)]
44. Gaisie, E.; Oppong-Yeboaha, N.Y.; Cobbina, P.B. Geographies of infections: Built environment and COVID-19 pandemic in metropolitan Melbourne. *Sustain. Cities Soc.* **2022**, *81*, 103838. [[CrossRef](#)] [[PubMed](#)]
45. Choi, K.H.; Denice, P. Socioeconomic Variation in the Relationship Between Neighbourhoods' Built Environments and the Spread of COVID-19 in Toronto, Canada. *Can. Stud. Popul.* **2022**, *49*, 149–181. [[CrossRef](#)]
46. Schmiede, D.; Haselhoff, T.; Ahmed, S.; Anastasiou, O.E.; Moebus, S. Associations Between Built Environment Factors and SARS-CoV-2 Infections at the Neighbourhood Level in a Metropolitan Area in Germany. *J. Urban Health* **2023**, *100*, 40–50. [[CrossRef](#)]
47. Wang, J.; Wu, X.; Wang, R.; He, D.; Li, D.; Yang, L.; Yang, Y.; Lu, Y. Review of Associations between Built Environment Characteristics and Severe Acute Respiratory Syndrome Coronavirus 2 Infection Risk. *Int. J. Environ. Res. Public Health* **2021**, *18*, 7561. [[CrossRef](#)]
48. Li, C.; Li, B.; Lei, S.; Long, L.; Ke, Q.; Li, L. Research progress on prevention and treatment of novel coronavirus pneumonia infection. *China Pharm.* **2020**, *23*, 1168–1174.
49. Yang, J.; Xu, J.; Hu, T.; Cao, J. Satisfaction and Demands of Indoor Space in the High-Density Residential Areas in the COVID-19 Era. *Buildings* **2022**, *12*, 660. [[CrossRef](#)]
50. Wu, Y.; Zuo, P.; Peng, C.; Zhu, X. Resilience Assessment and Its Association Characteristics of Urban Community for Public Health Emergencies: A Case Study of the Central District of Wuhan City. *Int. Urban Plan.* **2023**, *38*, 11–20. [[CrossRef](#)]
51. Navaratnam, S.; Nguyen, K.; Selvaranjan, K.; Zhang, G.; Mendis, P.; Aye, L. Designing Post COVID-19 Buildings: Approaches for Achieving Healthy Buildings. *Buildings* **2022**, *12*, 74. [[CrossRef](#)]
52. Wang, L.; Jia, Y.; Li, X.; Yang, X.M. Urban Spatial Intervention Strategies for Infectious Disease Prevention and Control. *Urban Plan.* **2020**, *44*, 13–20+32.
53. Hishan, S.S.; Ramakrishnan, S.; Qureshi, M.I.; Khan, N.; Hasan, N.; Al-Kumaim, S. Pandemic thoughts, civil infrastructure and sustainable development: Five insights from COVID-19 across travel lenses. *J. Talent. Dev. Excell.* **2020**, *12*, 1690–1696.
54. Dietz, L.; Horve, P.F.; Coil, D.A.; Fretz, M.; Eisen, J.A.; Van Den Wymelenberg, K. 2019 Novel Coronavirus (COVID-19) Pandemic: Built Environment Considerations To Reduce Transmission. *mSystems* **2020**, *5*, e00245-20. [[CrossRef](#)] [[PubMed](#)]
55. Qin, T.; Ruan, X.; Duan, Z.; Cao, J.; Liang, J.; Yang, J.; Jiang, Y.; Shi, M.; Xu, J. Wildlife-Borne Microorganisms and Strategies to Prevent and Control Emerging Infectious Diseases. *J. Biosaf. Biosecurity* **2021**, *3*, 67–71. [[CrossRef](#)]

56. Shenzhen City 2022 National Economic and Social Development Statistical Bulletin. Available online: http://tjj.sz.gov.cn/zwgk/zfxgkml/tjsj/tjgb/content/post_10577661.html (accessed on 14 September 2023).
57. Fang, Y.; Zhou, X.; Zhang, Q. The Construction of Densely-populated Communities in Shenzhen: Practice and Rethinking in the Post-pandemic Era. *Urban Insight* **2022**, *4*, 64–74. [CrossRef]
58. Shenzhen Municipal Government Open Data Platform. Available online: https://opendata.sz.gov.cn/data/dataSet/toDataDetails/29200_05800007 (accessed on 28 April 2023).
59. Futian District Government Online. Available online: <http://www.szft.gov.cn/> (accessed on 28 April 2023).
60. Wang, L.; Hu, Z.; He, L. Research on the Influencing Factors of Community Resilience in Shanghai Based on Analysis of the Pandemic Situation. *Urban Dev. Stud.* **2023**, *30*, 60–66.
61. Wang, L.; Liao, S.; Zhao, X.; Qian, F. Exploration of Approaches and Factors of Healthy City Planning. *Int. Urban Plan.* **2016**, *31*, 4–9. [CrossRef]
62. Harden, S.R.; Schuurman, N.; Keller, P.; Lear, S.A. Neighborhood Characteristics Associated with Running in Metro Vancouver: A Preliminary Analysis. *Int. J. Environ. Res. Public Health* **2022**, *19*, 14328. [CrossRef]
63. Sokadjo, Y.M.; Atchadé, M.N. The Influence of Passenger Air Traffic on the Spread of COVID-19 in the World. *Transp. Res. Interdiscip. Perspect.* **2020**, *8*, 100213. [CrossRef]
64. Zhao, S.; Shen, M.; Musa, S.S.; Guo, Z.; Ran, J.; Peng, Z.; Zhao, Y.; Chong, M.K.C.; He, D.; Wang, M.H. Inferencing Superspreading Potential Using Zero-Truncated Negative Binomial Model: Exemplification with COVID-19. *BMC Med. Res. Methodol.* **2021**, *21*, 30. [CrossRef] [PubMed]
65. Nakaya, T.; Fotheringham, A.S.; Brunson, C.; Charlton, M. Geographically Weighted Poisson Regression for Disease Association Mapping. *Stat. Med.* **2005**, *24*, 2695–2717. [CrossRef] [PubMed]
66. Waang, C. Selection of Optimal Significance Level α on Statistical Hypothesis Test. Master's Thesis, Lanzhou University of Finance and Economics, Lanzhou, China, 2013. Available online: <https://kns.cnki.net/KCMS/detail/detail.aspx?dbcode=CMFD&dbname=CMFD201302&filename=1013212553.nh&v=> (accessed on 20 April 2022).
67. O'Brien, R.M. A Caution Regarding Rules of Thumb for Variance Inflation Factors. *Qual. Quant.* **2007**, *41*, 673–690. [CrossRef]
68. Frank, L.D.; Wali, B. Treating Two Pandemics for the Price of One: Chronic and Infectious Disease Impacts of the Built and Natural Environment. *Sustain. Cities Soc.* **2021**, *73*, 103089. [CrossRef] [PubMed]
69. Li, T.; Wang, J.; Huang, J.; Gao, X. Exploring Temporal Heterogeneity in an Intercity Travel Network: A Comparative Study between Weekdays and Holidays in China. *J. Geogr. Sci.* **2020**, *30*, 1943–1962. [CrossRef]
70. Yin, C.; Shao, C.; Wang, X.; Xiong, Z.; Cui, W. Influence of land use mix on non-work travel behavior based on modified entropy index. *J. Beijing Jiaotong Univ.* **2018**, *42*, 92–97.
71. Li, B.; Zhang, L. The revelation of SARS outbreak to urban planning in China. *City Plan. Rev.* **2003**, *7*, 71–72.
72. Yang, J.; Shi, B.; Shi, Y.; Li, Y. Construction of A Multi-Scale Spatial Epidemic Prevention System in High-Density Cities. *City Plan. Rev.* **2020**, *44*, 17–24.
73. Zhou, Y.; Zhang, J.; Guo, S. Exploration and Reflection On the Research of Medical and Health Facilities Planning Standards In the Case of COVID-19 Epidemic. *City Plan. Rev.* **2020**, *44*, 55–60+84.

Disclaimer/Publisher's Note: The statements, opinions and data contained in all publications are solely those of the individual author(s) and contributor(s) and not of MDPI and/or the editor(s). MDPI and/or the editor(s) disclaim responsibility for any injury to people or property resulting from any ideas, methods, instructions or products referred to in the content.